Observations of Spatial Variations of Boundary Layer Structure over the Southern Great Plains Cloud and Radiation Testbed

J. M. HUBBE, J. C. DORAN, J. C. LILJEGREN, AND W. J. SHAW

Pacific Northwest National Laboratory, Richland, Washington

(Manuscript received 4 October 1996, in final form 10 February 1997)

ABSTRACT

Results from a field campaign to study the response of the planetary boundary layer to spatially varying surface conditions are presented. Radiosondes released at four locations with contrasting land use characteristics in the U.S. Department of Energy's Cloud and Radiation Testbed (CART) in Kansas and Oklahoma showed significant variations in mixed-layer depth, temperature, and water vapor mixing ratios over distances of 100–200 km. Using CART and radiosonde data, estimates of the surface sensible and latent heat fluxes are derived; the results from several methods are compared and a discussion of the similarities and differences in the values is given. Although substantial flux differences among the sites account for some of the variations in the boundary layer behavior, other features of the ambient meteorology and initial conditions appear to be equally important. Despite large changes in mixed-layer and surface-layer temperatures over scales of approximately 100 km, no evidence for temperature-induced secondary circulations was found. A simple scaling argument is presented that gives a possible reason for this absence.

1. Introduction

Over uniform surfaces the properties of the planetary boundary layer (PBL) are relatively well understood (e.g., Garratt 1992), but over nonuniform surfaces the picture is not as clear. Modifications to the structure and evolution of the PBL arising from spatially varying surface characteristics have attracted considerable attention in the last decade. Much of this attention may be attributed to the recognition of the importance of land surface descriptions in climate models and the desire to describe surface energy exchange mechanisms properly in those models. The subject is also interesting in its own right and is relevant to a host of boundary layer phenomena such as PBL growth rate, entrainment, boundary layer cloud formation, and nonclassical mesoscale circulations (Segal and Arritt 1992).

A related issue is the problem of accounting for subgrid-scale variability in surface conditions in models, such as climate codes, that run with relatively coarse resolution of a few hundred kilometers on a side. A number of numerical studies (e.g., Avissar and Chen 1993; Hong et al. 1995; Lynn et al. 1995; Pielke et al. 1991) have suggested that the failure to account for such variability may adversely affect the performance of such codes. However, in a study of the effects of variable surface sensible and latent heat fluxes on boundary layer properties over a 10^5 km^2 region in Oklahoma and Kansas, Zhong and Doran (1997) concluded that the effects of gradients in the ambient meteorological conditions were often likely to be more significant than the effects of spatially inhomogeneous fluxes. Although field campaigns such as HAPEX-MOBILHY (Hydrologic Atmospheric Pilot Experiment and Modélisation du Bilan Hydrique, Pinty et al. 1989) and BOREAS (Boreal Ecosystem-Atmosphere Study, Sellers et al. 1995) have provided valuable datasets, observations suitable for studying spatially varying surface fluxes and the consequent differences in boundary layer properties over scales of 100–200 km have remained relatively limited. This paper discusses results from a set of boundary layer and surface measurements taken for this purpose in the southern Great Plains of the United States during the summer of 1995. Consistent with the conclusions of Zhong and Doran (1997), which were based primarily on modeling results, the observations show that even when subgrid-scale variability in sensible and latent heat fluxes is large, other factors are likely to be equally important in determining PBL properties. This implies that the results of modeling studies that assume idealized distributions of surface characteristics or spatially uniform ambient conditions should be treated with caution and that a relaxation of these idealized conditions should yield results with wider applicability.

2. Experiment site and measurements

The Southern Great Plains (SGP) Cloud and Radiation Testbed (CART) is operated by the U.S. Department

Corresponding author address: J. C. Doran, Pacific Northwest National Laboratory, P.O. Box 999, MSIN K9-30, Richland, WA 99352. E-mail: jc_doran@pnl.gov

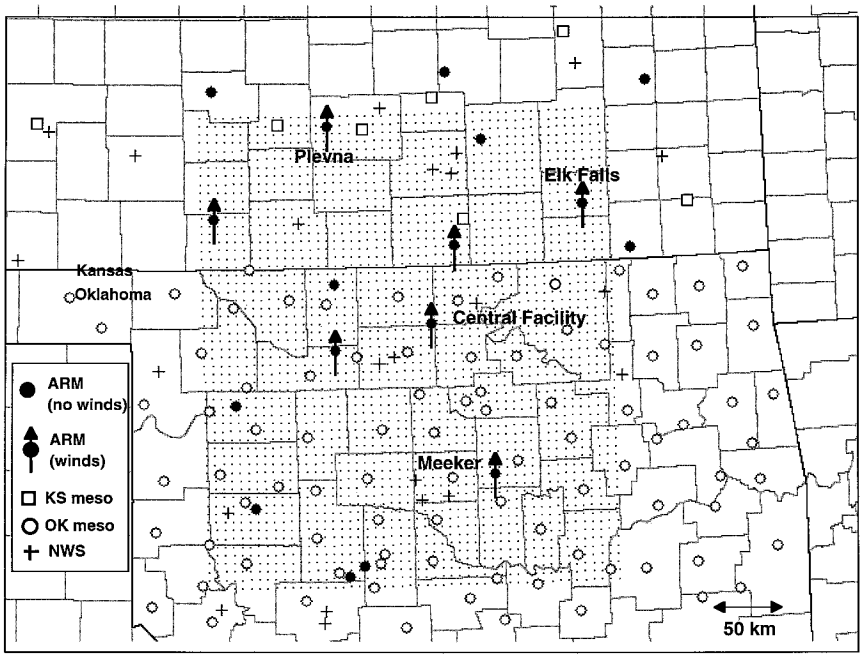

FIG. 1. Map of the CART and surrounding area showing locations of ARM extended facilities, Oklahoma Mesonet sites, Kansas Mesonet sites, and NWS sites. The computational grid used for flux calculations with the SiB2 model is shown overlaid on the CART domain. Temperatures were measured at all sites; winds were also measured at all sites except for the ARM locations indicated in the legend.

of Energy as part of its Atmospheric Radiation Measurement (ARM) program. It is situated in Kansas and Oklahoma and occupies an area of approximately 10^5 km^2. The SGP CART is one of the most heavily instrumented sites in the world for meteorological studies, and the ARM program routinely collects data not only from its own instruments distributed across the site but also from a variety of other sources, including the Oklahoma Mesonet, the Kansas State University network, and the National Weather Service. Among the instruments deployed at the CART in the summer of 1995 were 10 Bowen ratio stations that continuously recorded fluxes of sensible and latent heat. Data from this collection of instruments allow investigators to characterize the meteorology over the site in exceptional detail, especially near the surface where approximately 80 stations record temperature, wind, and humidity data at 1-h intervals or less.

Although the topography of the SGP CART is relatively simple, there are substantial differences in the surface characteristics across the domain arising primarily from variations in the local vegetation and from a substantial west–east gradient of precipitation. As shown below, these variations can lead to strong contrasts in the magnitudes of the surface sensible and latent heat fluxes across the CART, and these contrasts can be found with characteristic scales of 50 km or more. It seemed reasonable to expect that associated with these contrasts in surface properties would be corresponding differences in the behavior of the boundary layer over different regions of the CART. Accordingly, during the period 26 June through 13 July 1995 we conducted a field study to characterize some aspects of the behavior of the PBL in this area. Radiosondes were launched from three sites, Plevna, Elk Falls, and Meeker, with each site approximately 150 km from the CART central facility (Fig. 1). The sites were chosen to be representative of areas with significantly different vegetation characteristics. The Plevna site lies in relatively dry rangeland slightly north and east of a region heavily planted in winter wheat, which had been harvested by the time of our experiment. Elk Falls is in the northeast section of the CART, an area characterized by greater precipitation and by crops and native vegetation whose growing cycle extends considerably later into the year than that of winter wheat. Meeker is approximately 200 km south and slightly west of Elk Falls and is also east of the main winter wheat area. A Bowen ratio station was located within approximately 5 km of each of the sites from which the radiosondes were launched. The stations were located in areas nominally described as rangeland or pasture. Thus, the flux data from these instruments do not necessarily represent conditions over the general area because fluxes over cultivated fields in the region are not sampled. Nonetheless, a comparison of the data from the three stations provides a basis for at least a qualitative comparison of the surface fluxes near the various sites. Further details are provided below.

Radiosondes were launched six times per day at 0730, 0930, 1130, 1300, 1430, and 1600 LST, on 15 days during the experiment. The sondes measured wet- and dry-bulb temperatures and pressure. In addition, rawinsondes were launched from the central facility, located well within the winter wheat area at 0530, 0830, 1130, and 1430 LST. These soundings yielded a rich collection of data that can be used to relate boundary layer properties to varying surface and meteorological conditions. For this study we were interested primarily in studying factors affecting the growth of the mixed layer, and we chose two days, 7 and 12 July, for detailed examination. The spatial distributions of surface fluxes were similar (see below), but the evolution of the boundary layer over the CART differed substantially on these days.

The temperature sensors used in the radiosondes, manufactured by Atmospheric Instrumentation Research, Inc., were thermistors having a nominal accuracy of 0.5 K. Comparisons of the wet-and dry-bulb sonde temperatures obtained prior to adding water to the wet bulb wick showed generally good agreement between the two values. The dry-bulb sonde temperatures recorded just prior to launch were also compared with temperatures obtained from hand-held psychrometers. For sondes manufactured in 1994, mean biases in the dry-bulb temperatures ($T_{\text{psychrometer}} - T_{\text{sonde}}$) ranged between 0.5 K and 1.7 K for the three sites, with standard deviations of around 1 K. However, at the Meeker site, sondes obtained from a thermistor lot manufactured in 1995 showed a mean bias of 3.8 K with a standard deviation of 1.2 K. A second calibration point was obtained when the wick on the wet-bulb thermistor froze during the sondes' ascents. For the sondes manufactured in 1994, the indicated freezing temperatures averaged -0.9 K with a standard deviation of 0.2 K, with similar values found at all three sites. For the 1995 sondes, the corresponding values were -2.6 K and 0.6 K. Using these two sets of calibration points, a first-order adjustment of the 1995 sonde temperatures relative to the 1994 sonde temperatures was obtained by assuming a linear trend in the thermistors' temperature deviations between the two calibration points. For the cases presented here, only the Meeker flights at 1100, 1430, and 1600 LST on 7 July were affected. Although this adjustment procedure appeared to give generally satisfactory results, it is clear that one must exercise care when comparing temperature profiles from different radiosonde flights. In general, we believe that one must be prepared to accept an uncertainty of up to ± 1 K when comparing results from two different sondes. We comment on some implications of this uncertainty for our analysis later.

3. Boundary layer features

Figure 2 shows the 7 and 12 July soundings of potential temperatures θ obtained at the central facility and at the three sites from which radiosondes were released. The mixed-layer depth can be estimated from the depth of the layer in which the potential temperature is approximately constant. Although such an estimate for an individual sounding is subject to possible errors arising from the random sampling of individual convective plumes, a series of soundings can provide a reasonable description of the evolving boundary layer. Table 1 provides a summary of the estimated midafternoon mixed-layer depths derived from the profiles. Water vapor mixing ratio profiles (not shown) gave similar values for the mixed-layer depths. Note that the variation in depths on 7 July was relatively small while on 12 July the depths differed by as much as a factor of three or more. Moreover, on 12 July the mixed-layer potential temperatures at Plevna and the central facility were 5–6 K or more warmer than at Meeker and Elk Falls for most of the day. In contrast, on 7 July the midafternoon PBL potential temperatures differed by only a few kelvins among the four sites.

There are at least three local factors that influence the mixed-layer depths at the various sites on the different days: the ambient stability of the atmosphere, the strength and depth of the initial surface inversions, and the magnitudes of the surface sensible heat fluxes. For conditions in which advection is negligible and mechanical production of turbulence is small compared to buoyancy effects, Garratt (1992) gives a formula for the growth of the mixed layer

$$(h^2 - h_0^2) = 2\gamma_\theta^{-1}(1 + 2\beta) \int_0^t (\overline{w'\theta'})\, dt', \qquad (1)$$

where h is the depth of the boundary layer, h_0 is the initial depth, $\overline{w'\theta'}$ is the sensible heat flux at the surface, β is the ratio of the heat flux from entrainment at the top of the mixed layer to the surface heat flux, and γ_θ is the value of $d\theta/dz$ above the mixed layer.

On 12 July, the initial sounding at Plevna showed substantially less thermodynamic stability than the soundings at Elk Falls and Meeker. Above the initial surface inversion, the potential temperature at Plevna increased at a rate γ_θ of approximately 0.0010 K m^{-1} between 1500 and 3500 m AGL while at Elk Falls and Meeker the corresponding rate of increase was almost twice as large, 0.0019 K m^{-1}. The stability at the central facility was intermediate between that at Plevna and at the other two radiosonde sites. In addition, the early morning sounding at Plevna showed a residual mixed layer, between approximately 1400 and 2100 m AGL, whose potential temperature was nearly constant ($\gamma_\theta \approx 0$). This feature resulted in the rapid growth of the mixed layer between the 1300 and 1430 soundings when h reached this height range. Finally, at Plevna the surface inversion at 0730 was weaker and shallower than those at Elk Falls and Meeker, initially allowing a more rapid growth of the mixed layer for a given sensible heat flux at the surface. The differences in sensible heat fluxes at the various sites are discussed in the next section.

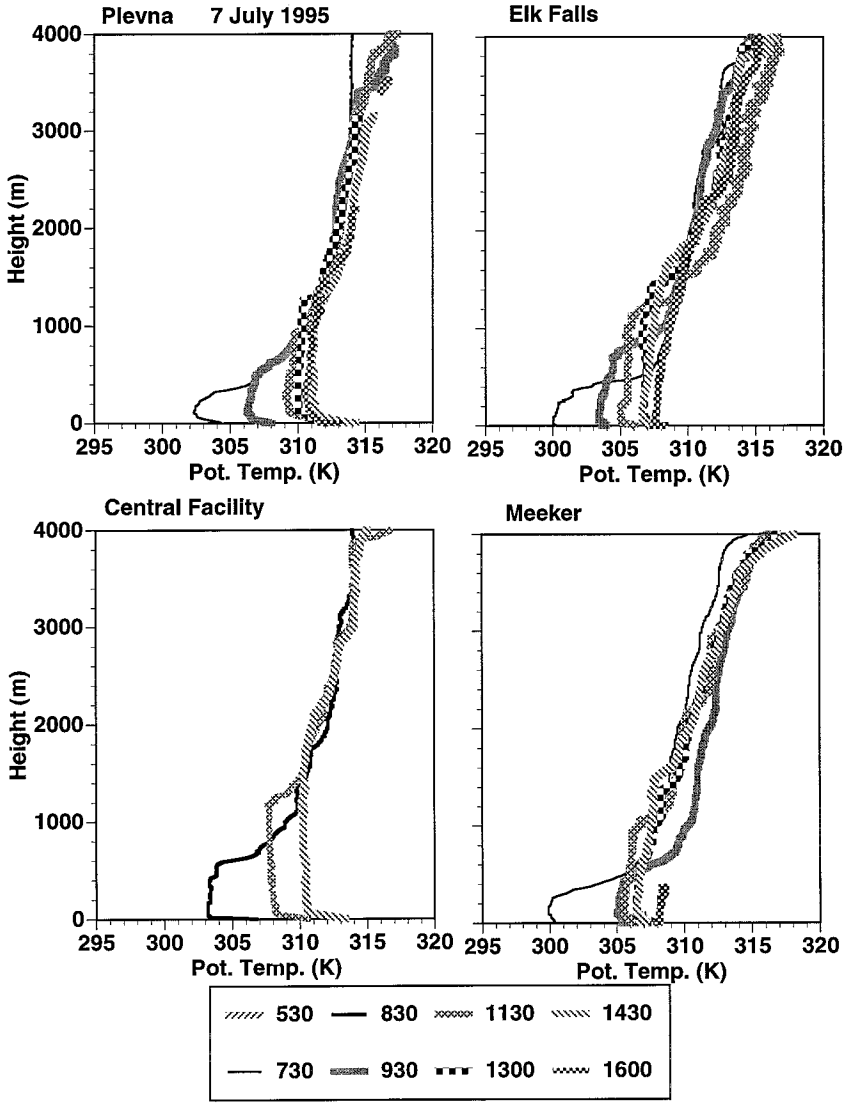

FIG. 2. Potential temperature soundings at four CART sites for (a) 7 July and (b) 12 July 1995.

Water vapor mixing ratio profiles had correspondingly large differences among the sites on 12 July. Above the mixed layers, values of approximately 6 g kg^{-1} were found at Plevna while Elk Falls and Meeker showed values of approximately 8 g kg^{-1}; near the surface these values increased to 9–12 kg^{-1} at Plevna and 15–18 kg^{-1} at Meeker and Elk Falls. Little or no cumulus development was observed at any of the sites. Even though there was significantly more water vapor in the lower atmosphere in the Elk Falls area than around Plevna, the absence of clouds implies that the afternoon lifting condensation levels were higher than the mixed layers in both regions. On 7 July similar differences among the sites were observed, but the moist layer at Elk Falls was significantly deeper than on 12 July.

4. Surface flux analysis

We employed three methods to estimate the magnitudes of the surface sensible heat fluxes that drive the growth of the boundary layer. In the first method we integrated $\rho C_p[\Delta\theta(z)/\Delta t]$ from the surface to a height sufficiently far above the surface that the temperature was no longer affected by surface fluxes or entrainment. Here, $\Delta\theta(z)/\Delta t$ is the change in potential temperature profiles determined from two radiosonde flights. If we define the quantity $I(z)$

$$I(z) = \int_0^z \rho C_p \frac{\Delta\theta(z')}{\Delta t}\, dz' \qquad (2)$$

and plot $I(z)$ as a function of height, then $I(z)$ should initially increase, decrease slightly as z passes through

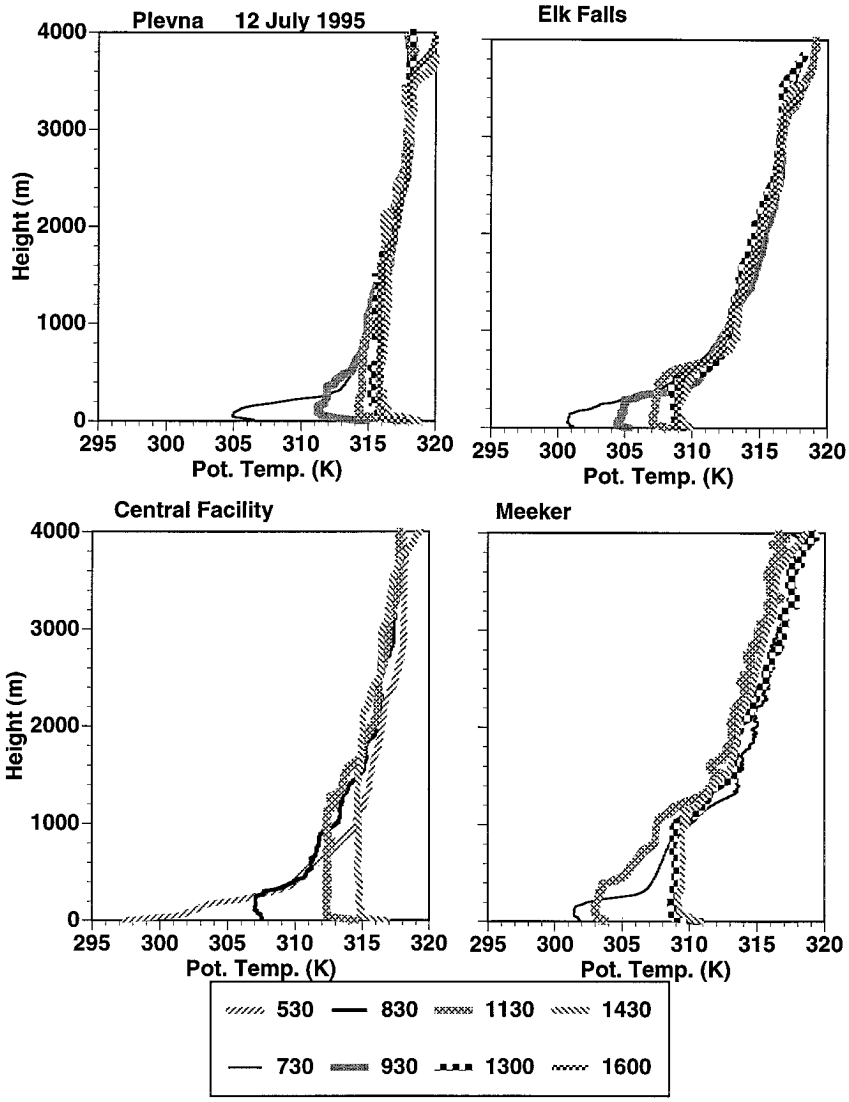

FIG. 2. (*Continued*)

the entrainment zone, and then level off above this height. If radiative and advective effects are negligible, this final value of $I(z)$ is then equal to the time average flux of sensible heat from the surface to the atmosphere.

The soundings of 7 July show too much temporal variation above the boundary layer at Meeker and Elk Falls to apply this method, but the soundings taken on 12 July appear to be suitable. The 12 July profiles at Plevna and Elk Falls show little change in potential temperature above approximately 2000 m during the course of the day, indicating that advective changes were small. Farther to the south at the central facility and at Meeker there were somewhat larger changes in the potential temperature values aloft that may reflect either advection or differences in calibrations of individual sondes. For the Meeker calculation we increased the 1430 sounding by 1 K at all levels. This attempt to adjust for possible effects of advection or calibration differences is admittedly somewhat ad hoc, but it does bring the 0730 and 1430 soundings into almost perfect correspondence between 1500 and 3500 m AGL and thus seems a reasonable correction.

TABLE 1. Midafternoon mixed-layer depths estimated from potential temperature profiles at four sites on 7 and 12 July 1995. All heights are in meters.

Site	Depth (7 July)	Depth (12 July)
Plevna	1300–1400	1800–2000
Elk Falls	1400–1600	500–600
Meeker	1300–1500	1100–1300
Central Facility	1700–1900	2000–2200

Figure 3 shows a plot of $I(z)$ versus z using the 0730 and 1430 soundings on 12 July to determine the changes in potential temperature over a 7-h period. The central facility did not have a sounding at 0730 so an equivalent

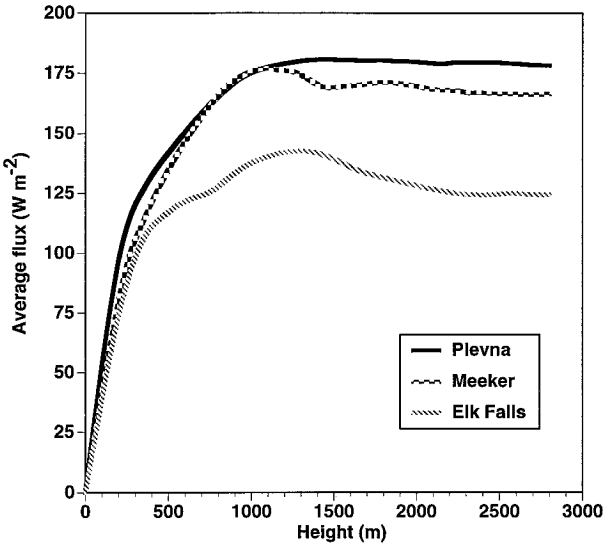

FIG. 3. On 12 July 1995 $\int_0^{z'} \rho C_p[\Delta\theta(z')/\Delta t]\, dz'$ as a function of z for three CART sites.

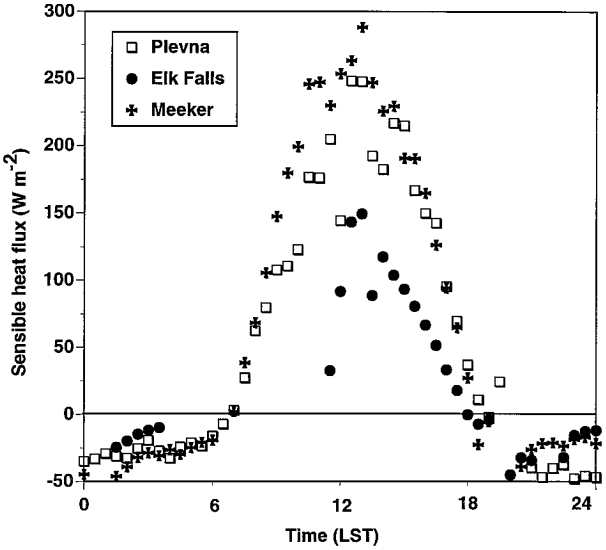

FIG. 4. Sensible heat fluxes from Bowen ratio measurements at three sites on 12 July 1995.

time average cannot be determined. All of the curves level off above approximately 2000 m, consistent with the description above, and they indicate that significantly higher average sensible heat fluxes occurred during this period at Plevna and Meeker than at Elk Falls. The values for each site are listed in Table 2. With the 1-K adjustment at Meeker, the average sensible heat fluxes at Meeker and Plevna are found to be nearly the same; without such an adjustment, the calculated Meeker flux is about two-thirds as large as at Plevna.

The second method for estimating surface heat fluxes used data from the Bowen ratio stations located near the radiosonde release points. Figure 4 shows time series of sensible heat flux values for the 12 July case. The peak values at Plevna and Meeker are nearly twice those found at Elk Falls. We calculated the area under the data points for the Meeker and Plevna sites to obtain the average sensible heat fluxes between 0730 and 1430 LST. To replace missing data for Elk Falls during much of the morning, we assumed a linear increase of flux from zero at 0730 LST to the first nonzero value that was recorded at 1130 LST. The results of this procedure are also given in Table 2. Although there is a Bowen ratio station at the central facility, it is located in a small pasture surrounded by wheat fields, and the fluxes measured by it are known to be unrepresentative of the general area. An eddy correlation instrument has since been added to obtain fluxes over a nearby wheat field but data from this instrument were not available at the time of our experiment.

Our third method of estimating fluxes over the CART site used a technique we have developed that applies the Simple Biosphere Model (SiB2) (Sellers et al. 1996) to a fine resolution grid to calculate fluxes from a knowledge of the vegetation, soil, and meteorological conditions. A full description of the technique will be published elsewhere, but a brief summary is given here.

SiB2 was run for the CART using grid cells of 6.25 km on a side. We use a multiquadric interpolation scheme (Nuss and Titley 1994) to determine the meteorological input parameters of temperature, pressure, humidity, wind speed, and insolation needed at each grid point to drive SiB2. The data to be interpolated were obtained from the data sources listed earlier, and precipitation data were also obtained from the Arkansas–Red Basin River Forecast Center's NEXRAD Stage III precipitation product. In all there are approximately 80 stations within the CART domain and nearly 150 total stations used in the various interpolations. SiB2 also requires a time-varying leaf area index (LAI) at each grid point to estimate the biophysical rates that control local evapotranspiration. We derive estimates of the LAI from the normalized difference vegetation index (NDVI) using a method described by Sellers et al.

TABLE 2. Time-averaged sensible heat fluxes from 0730 to 1430 LST 12 July 1995 evaluated by different methods. The last column is a SiB2 multielement average for 7 July 1995. All values are in watts per square meter.

Site	Radiosonde	SiB2 (single)	SiB2 (multi)	Bowen ratio	SiB2 7 July 95
Plevna	180	115	158	155	173
Elk Falls	125	15	52	56	32
Meeker	168	239	209	202	212
Central Facility	—	247	278	—	295

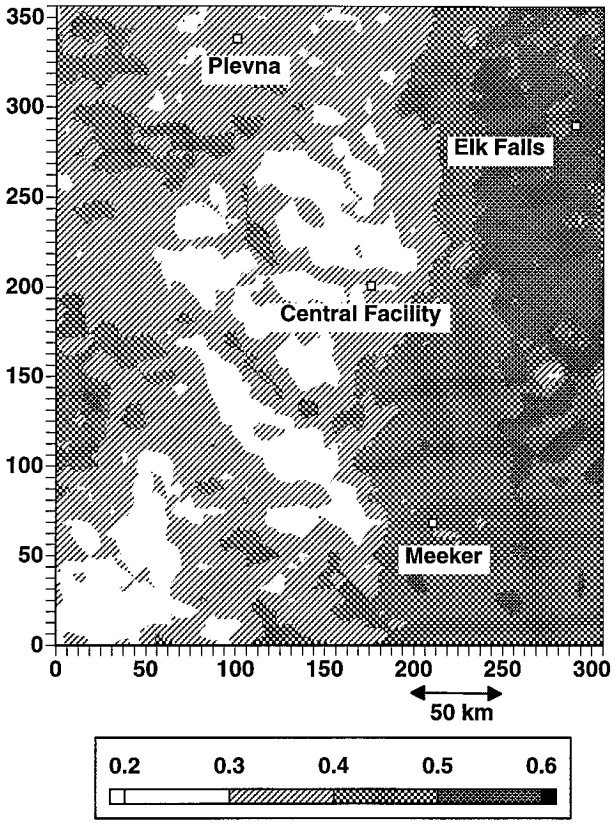

FIG. 5. Distribution of NDVI values over the CART on 9 July 1995.

(1994); the NDVI values are obtained from AVHRR imagery provided by ARM. During our measurement period the NDVI pattern did not change significantly, although there was some reduction in NDVI values over the central third of the domain. Figure 5 shows a map of the NDVI distribution over the area for 9 July 1995. Vegetation types for the CART are contained in a database generated by the U.S. Geological Survey (USGS 1990), and soil types are obtained from the STATSGO database and mapped into the USDA classifications described by Clapp and Hornberger (1978). Soil moisture was initialized at 65% of capacity at the end of January, and the model was then run through the end of July. After the entire area had experienced significant precipitation, which occurred within the first month, the results of the simulations were generally insensitive to the initial soil moisture distribution.

Another important factor affecting the fluxes is the variation in precipitation over the site. The first part of the experiment had significant precipitation over large areas of the domain while the last nine days were generally much drier. As a result, during the last week of our measurements the flux contrasts across the site were substantially larger than during the first week. Figure 6 shows distributions of sensible heat fluxes over the CART at 1300 LST for 7 and 12 July; the flux patterns on these two days are quite similar. The contrasts in flux values among different regions of the domain reflect both the contrasts in the state of the vegetation and in the available soil moisture.

We have used the SiB2 model to calculate fluxes for the grid element nearest each of the radiosonde release points as well as for the 5×5 element areas over and upwind of each release site. The average fluxes from 0730 to 1430 LST for these single element and multielement areas are also given in Table 2. The last column of the table gives the multielement average for the 7 July case as well.

As can be seen in Table 2, there are differences in the average sensible heat flux values obtained by the various methods of estimation, which is hardly surprising considering that each approach samples a different area with different surface characteristics. For the Plevna and Meeker sites, the multielement SiB2 values agree with the radiosonde values to within 24% or better, which is encouraging. The discrepancy is significantly larger at the Elk Falls site, where the interpolated net radiation field used to drive SiB2 showed evidence of cloudiness during the morning hours even though a local observer reported clear skies. The reduced radiation available for partitioning into sensible and latent heat fluxes probably accounts for some of the difference between the SiB2 and the radiosonde results, but we have also experienced some difficulties with the SiB2 model applied at these scales. For example, we have found that SiB2 shows some problems in reproducing the proper timing for the increase and decrease of the surface fluxes. There are also indications that failing to account for changes in the relative populations of vegetation biomes during the course of a growing season results in degraded model performance during multimonth simulations. Nonetheless, the approach shows considerable promise for obtaining distributions of fluxes over the whole CART region. In particular, it provides a means of comparing the patterns and relative magnitudes of sensible and latent fluxes over the CART on different days, which is especially useful for our current purposes (see below).

Note that comparisons of fluxes derived from Bowen ratios with fluxes derived from the other two methods may be misleading because the former values apply to much smaller spatial scales than the latter. Thus, the good agreement between the fourth and fifth columns of the table is probably fortuitous. The Bowen ratio data have been useful, however, for evaluating the performance of the SiB2 model when the model is applied to the region immediately surrounding the Bowen ratio site. The similarities and discrepancies among the various flux estimates illustrate some of the difficulties involved in ascertaining what flux values should be used in areas of nonuniform surface characteristics when evaluating or driving a mesoscale model.

The flux values listed in Table 2 indicate that the Elk Falls site is located in an area with significantly smaller

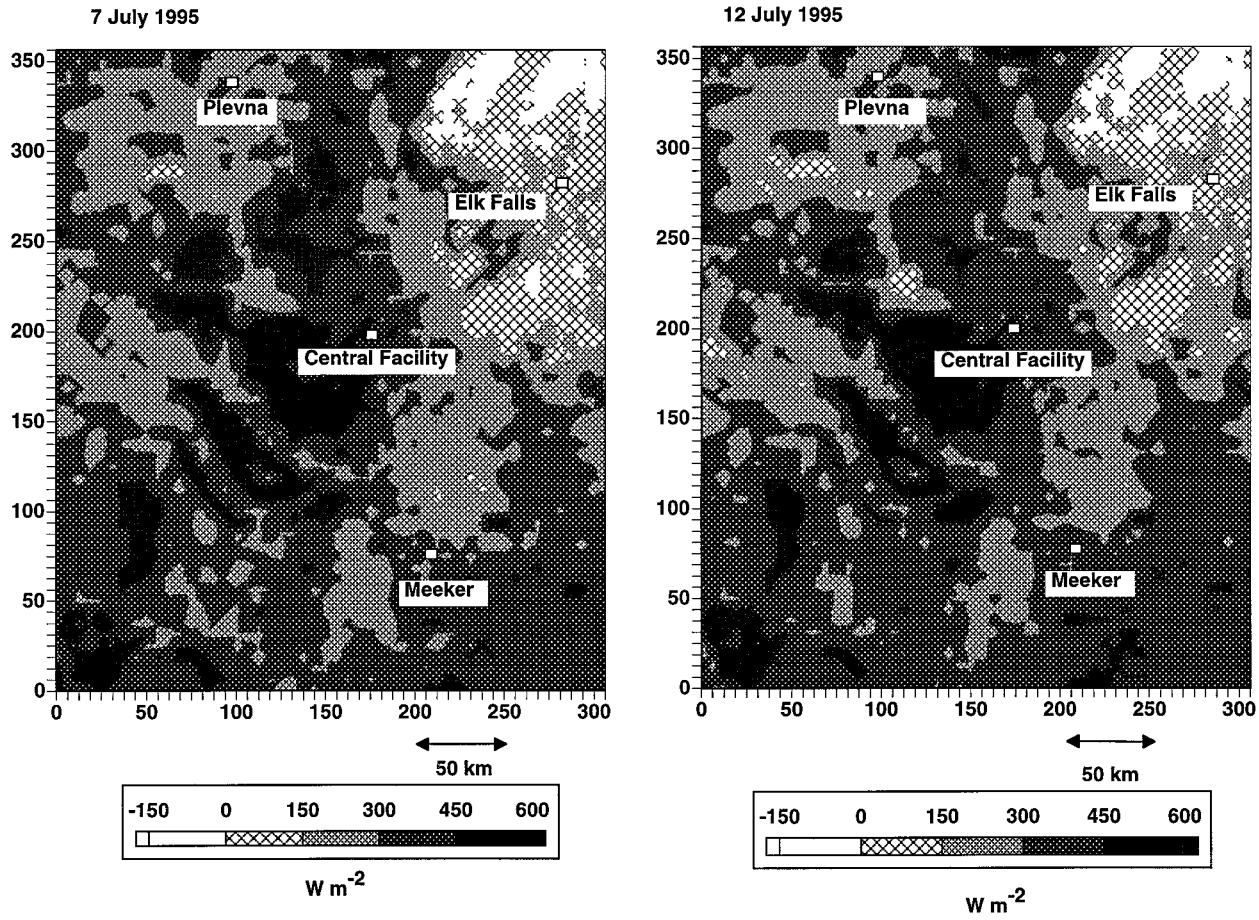

FIG. 6. Distribution of sensible heat fluxes over the CART calculated with the SiB2 model at 1300 LST for (a) 7 July and (b) 12 July 1995.

sensible heat fluxes and larger latent heat fluxes (not shown) than Plevna, Meeker, or the central facility. Although there are substantial flux contrasts among various regions of the CART, an examination of the values given in Tables 1 and 2 shows that the differences in mixed-layer depths on 12 July are larger than can be explained by differences in surface fluxes alone. If we use the multielement SiB2 fluxes as representative values and assume that all other conditions were equal, then the central facility should have had the largest mixed-layer depth while the depth at Elk Falls should have been approximately 40% as large. This is clearly not what was observed at Elk Falls. It is also worth noting the differing evolution of the mixed layer on 7 and 12 July. Even though the flux patterns determined with the SiB2 model were similar on the two days, the growth of the mixed layer at the three radiosonde locations was not. The mixed-layer depths on July showed less variation, indicating that factors other than the local sensible heat fluxes must have played a strong role in determining the growth of the mixed layer, particularly at Elk Falls where the sensible heat fluxes were small. We have already noted the different ambient stabilities over the radiosonde sites, and advection from warmer or cooler regions undoubtedly also plays an important role. Such behavior shows the potential pitfalls of focusing on flux comparisons without considering differences in the ambient meteorology, initial conditions, and nonlocal influences when comparing boundary layer properties, as may be done in more idealized numerical exercises.

5. Mesoscale circulations

The development of mesoscale circulations over regions of contrasting surface sensible heat fluxes has been a subject of interest for some time. Probably the best known examples of thermally induced winds are sea and land breezes, which can form regularly in coastal areas when land–water temperature contrasts are favorable. In recent years, there has also been substantial interest in nonclassical mesoscale circulations (NCMCs) induced by contrasts in land surface characteristics attributable to factors such as vegetation or soil moisture differences (Segal and Arritt 1992). Although numerous numerical modeling studies have indicated the potential

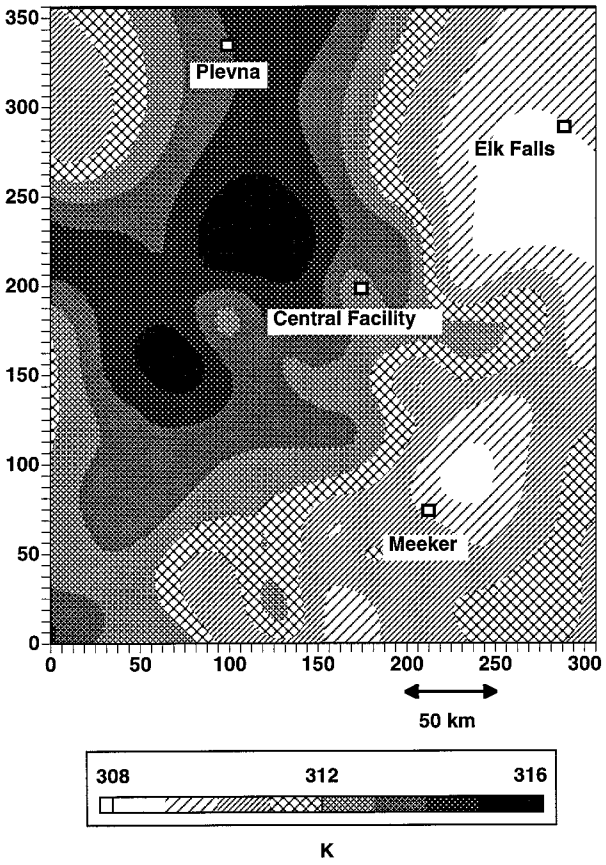

FIG. 7. Contours of interpolated surface air temperatures at 1300 LST 12 July 1995.

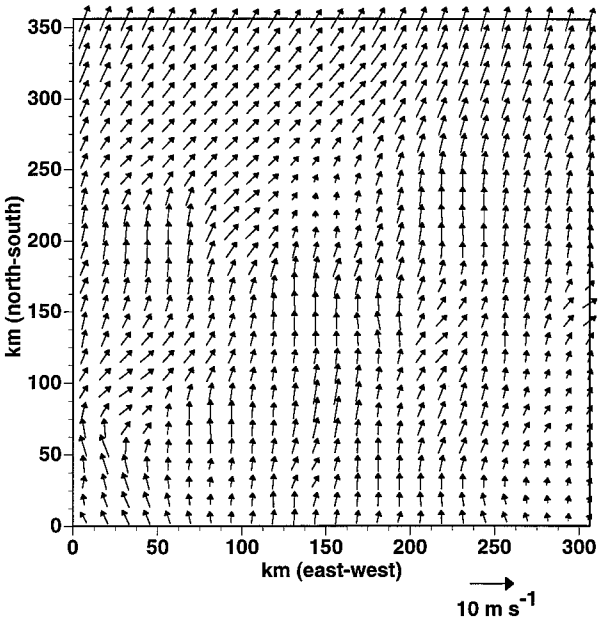

FIG. 8. Vector plot of interpolated surface winds at 1300 LST 12 July 1995.

importance of such NCMCs, the experimental evidence for them, on scales on the order of 100 km, remains meager (Zhong and Doran 1997). Segal et al. (1991) showed evidence for a ''snow breeze'' but vegetation and soil moisture influences appear to be generally weak.

The conditions encountered on 12 July 1995 at the SGP CART seemed particularly favorable for the development of NCMCs. Wind speeds near the surface averaged less than 4 m s^{-1} until 1400 LST and less than 5 m s^{-1} until 1630 LST. As noted above, the potential temperature soundings at Plevna and Elk Falls showed differences of 5–6 K or more in the BL potential temperatures from 0930 on. We used the interpolated fields needed for our SiB2 calculations to examine the distribution of surface air temperatures across the CART; the results of this analysis (Fig. 7) are consistent with the sounding data, showing temperature differences of 6–7 K among different regions of the CART. We then attempted to identify NCMCs by displaying the interpolated near-surface wind fields over the CART, animating the display, and looking for evidence of the wind turning to blow from cooler to warmer areas. An examination of the winds showed no obvious patterns that can be identified as NCMCs. While it was possible to find regions in which transient occurrences of convergence developed, we were not able to associate these regions unambiguously with corresponding temperature gradients. Figure 8 shows an example of the interpolated near-surface wind field at 1300 LST 12 July. Even though there were strong temperature contrasts present, there is little evidence for the development of an NCMC at this or other times.

In an earlier study at a similar scale, Segal et al. (1989) attributed the absence of a readily identified NCMC to the influence of terrain effects and synoptic winds. In a study at smaller scales, Zhong and Doran (1995) also pointed out the importance of topography in masking the appearance of an NCMC. It is unlikely that either of these factors were important in the current case. The prevailing winds on 12 July were from the south, relatively light, and perpendicular to the direction in which thermally induced circulations might have been expected to develop because the temperature gradients were primarily from east to west. Moreover, the terrain is generally higher to the west so that upslope winds developing during the day would have strengthened winds arising from sensible heat flux contrasts. It is possible that the density of observing stations was not sufficient to reveal the development of an NCMC if only weak local flows developed. Moreover, although the combination of ambient winds and the limited extent of significantly hotter or cooler areas might limit the development of an NCMC, based on an analysis of Segal et al. (1988), we believe another mechanism may also contribute.

In their work, Segal et al. (1988) evaluated the circulation around a path spanning two regions with dif-

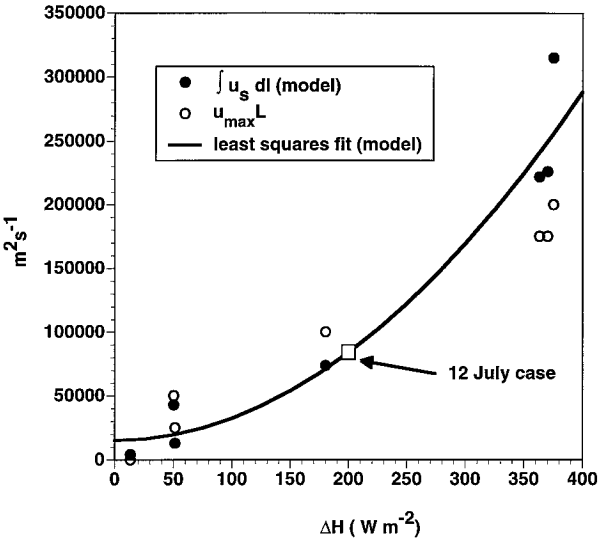

FIG. 9. Comparison of $\int u_s\, dl$ and $u_{max}L$ as a function of ΔH. Values of $\int u_s\, dl$ and $u_{max}\, L$ are from the model results of Segal et al. (1988), with $L = 25$ km, and the solid line is a least squares quadratic fit to the $\int u_s\, dl$ values. The open square represents the approximate conditions over the CART for 12 July 1995.

ferent surface sensible heat fluxes. With a suitable choice of path, the circulation reduces to the quantity $\int u_s\, dl$, where u_s is the surface wind component induced by differential heating over two land surfaces and l is the pathlength over which u_s is evaluated. Using a two-dimensional mesoscale model, they showed that this integral is essentially a function of the difference in the maximum heat flux ΔH in the two adjacent regions over which the secondary circulation develops. We can use these results to obtain a useful estimate of the expected magnitude of the thermally induced winds over the CART. We do this by assuming that the integral can be approximated with the expression $u_{max}L$, where u_{max} is the maximum velocity of the secondary circulation u_s and L is some characteristic scale length. Inspection of several of the figures of Segal et al. (1988) shows that the maximum values of u_{max} range between approximately 1 and 8 m s^{-1}, and that the horizontal temperature changes (1–6 K) in the mixed layer typically occur over a distance of 20–30 km. If we use this latter feature to choose a scale length of 25 km, we can then compare the variation of $u_{max}L$, as a function of ΔH, with the variation of $\int u_s\, dl$. The results are shown in Fig. 9 for conditions 6 h after the onset of thermal circulations and assuming a sinusoidal variation in heat flux; a least squares quadratic fit to the model values is also shown. The circulation data for this figure are listed in Table 9 of Segal et al. (1988). The figure shows that $u_{max}L$ provides a reasonable estimate of the circulation.

To apply this result to the CART, we note from Figs. 2 and 7 that the maximum temperature differences over the CART are approximately 6–7 K, similar to the maximum value found in Segal et al. (1988), but occur over distances on the order of 100 km rather than 25 km. If we use the results from Fig. 6 and Table 2 to estimate $\Delta H \leq 200$ W m^{-2}, and if we assume a scale length of 100 km, based on the distance over which large temperature changes occur, then we can estimate $u_{max} < 1$ m s^{-1}. Even if $\Delta H \sim 325$ W m^{-2}, u_{max} would still be less than 2 m s^{-1}. This result implies that any NCMC found over the CART domain would have been quite weak despite the large differences in temperatures found between the Elk Falls and Plevna regions.

Strictly speaking, this type of scale analysis is applicable to a two-dimensional domain with land use patterns of the type considered by Segal et al. and not to the distribution of surface characteristics found in the CART. Nevertheless, the results suggest one reason why NCMCs in nature are apt to be less significant than those found in idealized simulations. In the case of a sea breeze or a vegetation breeze induced by *abrupt* changes in land-surface characteristics (which are then maintained for considerable distances), a significant NCMC can be expected to develop. However, when the changes in land-surface characteristics occur over a longer distance, which is the case at the CART and which is likely to be more common in real-world conditions, NCMCs can be expected to be considerably weaker. This behavior may also help to explain why Segal et al. (1989) did not detect significant NCMCs over northeastern Colorado in their study even though surface infrared temperatures showed noontime contrasts of approximately 10 K. It would be useful to carry out a series of numerical experiments to test this hypothesis more thoroughly.

These conclusions are consistent with those of Zhong and Doran (1997), who suggested that secondary circulations generated by land use differences are unlikely to be as significant in nature as might have been concluded on the basis of numerical experiments using highly idealized surface conditions. As a result, we believe that the utility of modeling studies that focus on idealized land-surface and meteorological conditions to illustrate the importance of land-surface contrasts may be significantly improved by explicitly considering spatial variations in the initial and ambient meteorological conditions and by using more realistic spatial distributions of land-surface characteristics.

6. Summary

We carried out a series of radiosonde releases at four sites in the DOE's CART in Oklahoma and Kansas. The sites were located in regions with substantially different surface characteristics due, in part, to the harvest of extensive areas of winter wheat earlier in the year and to spatial variations in rainfall over the region. On one day, variations in mixed-layer heights of over a factor of three were found among the sites, and horizontal potential temperature contrasts in the mixed layer of 6–7 K were observed. An analysis of surface temperature

observations independently confirmed the existence of these large temperature contrasts over distances of the order of 100 km. The variations in mixed-layer depths from site to site were attributed to differences in ambient stability, the depth and strength of the initial surface inversion, and the magnitude of the surface sensible heat fluxes, with the first two factors appearing to be as important as the third. Sensible heat fluxes were estimated at three sites by vertically integrating the changes in potential temperature in two soundings taken 7 h apart during a period with little or no advective changes to the temperature. Fluxes were also measured by Bowen ratio stations located near the radiosonde release points and by applying the SiB2 model to the full CART at a resolution of 6.25 km. Each technique yielded fluxes characteristic of different scales, complicating comparisons of the values, but there are some general areas of agreement.

Using scaling arguments derived from simulations by Segal et al. (1988) to relate the strength of secondary circulations to differences in the heat fluxes between two areas, we found that secondary circulations are likely to be weak in this region despite large temperature contrasts between the observation sites. This is consistent with results obtained from interpolations of the observed near-surface wind fields. The weakness of such circulations and the significant roles played by initial and ambient meteorological conditions in determining boundary layer characteristics are also consistent with recent observational and modeling analyses. Numerical simulations using more realistic land surface characteristics and meteorology are recommended.

Acknowledgments. We thank Larry Berg, Lorenzo de la Fuente, Edi Santoso, and Marcus Buker for conducting the radiosonde measurements, and Prof. Roland Stull for making the necessary arrangements for their participation. This research was supported by the Environmental Sciences Division of the U.S. Department of Energy under Contract DE-AC06-76RLO 1830 at Pacific Northwest National Laboratory under the auspices of the Atmospheric Radiation Measurement Program. Pacific Northwest National Laboratory is operated for the U.S. Department of Energy by Battelle Memorial Institute.

REFERENCES

Avissar, R., and F. Chen, 1993: Development and analysis of prognostic equations for mesoscale kinetic energy and mesoscale (subgrid scale) fluxes for large-scale atmospheric models. *J. Atmos. Sci.,* **50,** 3751–3774.

Clapp, R. B., and G. M. Hornberger, 1978: Empirical equations for some soil hydraulic properties. *Water Resour. Res.,* **14.4,** 601–604.

Garratt, J. R., 1992. *The Atmospheric Boundary Layer*. Cambridge University Press.

Hong, X., M. J. Leach, and S. Raman, 1995: A sensitivity study of convective cloud formation by vegetation forcing with different atmospheric conditions. *J. Appl. Meteor.,* **34,** 2008–2028.

Lynn, B. H., D. Rind, and R. Avissar, 1995: The importance of mesoscale circulations generated by subgrid-scale landscape heterogeneities in general circulation models. *J. Climate,* **8,** 191–205.

Nuss, W. A., and D. W. Titley, 1994: Use of multiquadric interpolation for meteorological objective analysis. *Mon. Wea. Rev.,* **122,** 1611–1631.

Pielke, R. A., G. A. Dalu, J. S. Snook, T. J. Lee, and T. G. F. Kittel, 1991: Nonlinear influence of mesoscale land use on weather and climate. *J. Climate,* **4,** 1053–1069.

Pinty, J.-P., P. Mascart, E. Richard, and R. Rosset, 1989: An investigation of mesoscale flows induced by vegetation inhomogeneities using an evapotranspiration model calibrated against HAPEX-MOBILHY data. *J. Appl. Meteor.,* **28,** 976–992.

Segal, M., and R. W. Arritt, 1992: Nonclassical mesoscale circulations caused by surface sensible heat-flux gradients. *Bull. Amer. Meteor. Soc.,* **73,** 1593–1604.

——, R. Avissar, M. C. McCumber, and R. A. Pielke, 1988: Evaluation of vegetation effects on the generation and modification of mesoscale circulations. *J. Atmos. Sci.,* **45,** 2268–2292.

——, W. E. Schreiber, G. Kallos, J. R. Garratt, A. Rodi, J. Weaver, and R. A. Pielke, 1989: The impact of crop areas in northeast Colorado on midsummer mesoscale thermal circulations. *Mon. Wea. Rev.,* **117,** 809–825.

——, J. H. Cramer, R. A. Pielke, J. R. Garratt, and P. Hildebrand, 1991: Observational evaluation of the snow breeze. *Mon. Wea. Rev.,* **119,** 412–424.

Sellers, P. J., C. J. Tucker, G. J. Collatz, S. O. Los, C. O. Justice, D. A. Dazlich, and D. A. Randall, 1994. A global 1° by 1° NDVI data set for climate studies. Part 2: The generation of global fields of terrestrial biophysical parameters from the NDVI. *Int. J. Remote Sens.,* **15,** 3519–3545.

——, and Coauthors, 1995: The Boreal Ecosystem–Atmosphere Study (BOREAS): An overview and early results from the 1994 field year. *Bull. Amer. Meteor. Soc.,* **76,** 1549–1577.

——, and Coauthors, 1996: A revised land surface parameterization (SiB2) for atmospheric GCMs. Part I: Model formulation. *J. Climate,* **9,** 676–705.

SGS, 1990: Prototype 1990 conterminous U.S. land cover characteristics data set CD-ROM. EROS Data Center.

Zhong, S., and J. C. Doran, 1995: A modeling study of the effects of inhomogeneous surface fluxes in boundary-layer properties. *J. Atmos. Sci.,* **52,** 3129–3142.

——, and ——, 1997: A study of the effects of spatially varying fluxes on cloud formation and boundary-layer properties using data from the southern Great Plains cloud and radiation testbed. *J. Climate,* **10,** 327–341.